Salt stress in *Desulfovibrio vulgaris* Hildenborough: An integrated genomics approach.

Aindrila Mukhopadhyay[1,2], Zhili He[1,4], Eric J. Alm[1,2], Adam P. Arkin[1,2,7], Edward E. Baidoo[1,2], Sharon C. Borglin[1,3], Wenqiong Chen[1,6], Terry C. Hazen[1,3],Qiang He[1,4], Hoi-Ying Holman[1,3], Katherine Huang[1,2], Rick Huang[1,3], Dominque C. Joyner[1,3], Natalie Katz[1,3],Martin Keller[1,6], Paul Oeller[1,6],Alyssa Redding[1,7], Jun Sun[1,6], Judy Wall[1,5], Jing Wei[1,6], Zamin Yang[1,4], Huei-Che Yen[1,5], Jizhong Zhou[1,4], Jay D. Keasling[1,2,7*].

[1]Virtual Institute of Microbial Stress and Survival, [2]Physical Biosciences Division, Lawrence Berkeley National Laboratory, Berkeley, USA, [3]Earth Sciences Division, Lawrence Berkeley National Laboratory, Berkeley, USA, [4]Environmental sciences Division, Oak Ridge National Laboratory, Oak Ridge, Tennessee, USA, [5]Biochemistry and the Molecular Microbiology & Immunology Departments. University of Missouri, Columbia, USA, [6]Diversa Inc, San Diego, USA, [7]Departments of Chemical Engineering and Bioengineering, University of California, Berkeley, USA

*****Corresponding author

Prof. Jay D. Keasling

Berkeley Center for Synthetic Biology,

717 Potter Street, Berkeley, CA, 94720 USA

Email: keasling@berkeley.edu

Phone: 510-495-2620, Fax: 510-495-2630

DISCLAIMER

Abstract:

Recent interest in the ability of *Desulfovibrio vulgaris* Hildenborough to reduce, and therefore contain, toxic and radioactive metal waste, has made all factors that affect its physiology of great interest. Increased salinity constitutes an important and frequent fluctuation faced by *D. vulgaris* in its natural habitat. In liquid culture, exposure to excess salt resulted in a striking cell elongation in *D. vulgaris*. Using data from transcriptomics, proteomics, metabolite assays, phospholipid fatty acid profiling, and electron microscopy, we undertook a systems approach to explore the effects of excess NaCl on *D. vulgaris*. This study demonstrates that import of osmoprotectants such as glycine betaine and ectoine constitute the primary mechanism used by *D. vulgaris* to counter hyper-ionic stress. Several efflux systems were also highly up-regulated, as was the ATP synthesis pathway. Increase in both RNA and DNA helicases suggested that salt stress had affected the stability of nucleic acid base pairing. An overall increase in branched fatty acids indicated changes in cell wall fluidity. An immediate response to salt stress included up-regulation of chemotaxis genes though flagellar biosynthesis was down-regulated. Other down-regulated systems included lactate uptake permeases and ABC transport systems. The extensive NaCl stress analysis was compared with microarray data from KCl stress and unlike many other bacteria, *D. vulgaris* responded similarly to the two stresses. Integration of data from multiple methods has allowed us to present a conceptual model for salt stress response in *D. vulgaris* that can be compared to other microorganisms.

Introduction

Originally isolated in 1946 from clay soils in Hildenborough, Kent (UK), *Desulfovibrio vulgaris* Hildenborough belongs to the sulfate-reducing class of bacteria (SRB), found ubiquitously in nature (22, 43). These anaerobes generate energy by reducing sulfate (40) and play an important roles in global sulfur cycling and complete mineralization of organic matter. *D. vulgaris* has been implicated in bio-corrosion of oil and gas pipelines both on land and in the ocean (5, 22, 55). Members of this species have also been found to reduce metals in sediments and soils with high concentrations of NaCl and a milieu of toxic metals (6) and to cope with salt stresses that result from environmental hydration/dehydration cycles. An understanding of the ability of *D. vulgaris* to survive high NaCl and osmotic stress will be critical to discern the biogeochemistry at metal contaminated sites for bioremediation/natural attenuation and to predict the potential for bio-corrosion of pipelines and tanks in soils, sediments, and off-shore oil production (8, 36, 60). Availability of an annotated genomic sequence for *D. vulgaris* makes it ideal for the study of complex SRB physiology (24).

The bacterial response to hyper-ionic stress includes a range of mechanisms, such as aquaporins for water intake and functions regulated by the stationary phase sigma factor, RpoS (12, 51). A commonly encountered response is accumulation of neutral, polar, small molecules such as glycine betaine (GB), proline, trehalose, or ectoine (19, 28, 31). These compatible solutes serve as osmoprotectants and are synthesized and/or imported into the cell. The genomic sequence of *D. vulgaris* provides insight into its potential responses to increased salt in the environment. While genes for trehalose synthesis (*otsBA*) exist in the closely related microbe *Desulfovibrio* G20, homologues are

not present in *D. vulgaris*. Furthermore, no genes for ectoine synthesis or transport are identifiable. *D. vulgaris* does contain genes for proline biosynthesis and an ABC transport system annotated for the uptake of GB/choline/proline.

Compared to hyper-ionic stress, responses specific to Na^+ stress are less understood, since they are often observed in conjunction with osmotic or alkaline stress (14). RpoS-regulated genes have also been found to be responsive to Na^+ stress (12, 18). Also often implicated are Na^+/H^+ antiporters, such as those encoded by *nha* genes in *E. coli* (14, 54), orthologs of which are present in *D. vulgaris*.

A comprehensive understanding of various stress response mechanisms required the use of multiple techniques, addressing changes in different types of biomolecules. Integrated analysis combining microarray data and proteomics are increasingly being explored for studies at a cellular level. Although mRNA and protein levels are linked, additional regulation during and after translation require that expression at both stages be monitored for a more complete view of the physiological landscape (3, 23, 38). Though not addressed here, critical information of cellular proteomic response also lies in post transalational modifications. In this study, changes in the transcript and protein levels are presented. These data sets have been complemented by preliminary metabolite analysis. In addition, phospholipid fatty acid (PLFA) composition and lipid content, which are measures of changes in cell membrane properties, have also been studied.

Materials and Methods

Culture Maintenance *Desulfovibrio vulgaris* Hildenborough (ATCC29579) was obtained from American Type Culture Collection (Manassas, VA). All experiments and

culture maintenance used a defined lactate sulfate medium (LS4D) based on Postgate's Medium C (48). LS4D medium (1 L), pH 7.2, contains 50 mM $NaSO_4$, 60 mM sodium lactate, 8 mM $MgCl_2$, 20 mM NH_4Cl, 2.2 mM K_2PO_4, 0.6 mM $CaCl_2$, 30 mM PIPES buffer, 640 µl Resazurin (0.1% solution), 10 mM NaOH, 1ml Thauers vitamins (10), 12.5ml trace minerals (10), and 5ml titanium citrate. To prepare titanium citrate 500 ml of 0.2 M Sodium citrate was boiled for 20 min under a continuous stream of nitrogen to remove dissolved oxygen. While hot, 37.5 ml of 20 % (wt/vol) $TiCl_3$ was added along with 100 ml of 8% (wt/vol) Na_2CO_3 under nitrogen. The final mixture was autoclaved and used. Subculturing was minimized by using -80^oC *D. vulgaris* stocks as 10% inoculum into 100-200ml of fresh LS4D medium as a starter culture at mid-log phase growth (OD_{600} 0.3 – 0.4). This culture was then used as 10% inoculum into 1-3 liter production cultures. All growth was conducted at 30°C.

Minimum Inhibitory Concentration (MIC) MIC was defined as the stressor concentration that doubled the generation time and/or decreased the overall yield by 50%. Growth curves were conducted in 96-well plates using the OmniLog® instrument (Biolog Inc., Hayward, CA) which captured digital optical density images every 15min for 150 h. Each well was inoculated with 10% mid-log phase cells, with six replicates of each stressor dilution and the plates were sealed in an anaerobic atmosphere in airtight Retain bags (Nasco) before being placed in the OmniLog. OmniLog measurements were calibrated against *D. vulgaris* cell densities as measured at OD_{600}, a Biolog plate reader OD_{590}, and direct cell counts using the Acridine orange direct count (AODC) method. All growth curves were comparable at 95% confidence interval for exponential growth phase.

A kinetic plot of *D. vulgaris* growth was used to determine generation time and cell yield. For NaCl and KCl stress, the MIC for *D. vulgaris* was established to be 250 mM (additional to that present in LS4D) by testing concentrations from 0 to 5000 mM. For all experiments in this study, 250 mM NaCl or KCl was added to growth medium to establish stress conditions.

Biomass Production Highly controlled and reproducible conditions were used for simultaneous production of cell culture for transcriptomics, proteomics, metabolite assays, PLFA and synchrotron Fourier transform infrared spectromicroscopy (sFTIR) studies. Control and experimental production cultures were prepared in triplicate. Exposure to stress was done at mid-log phase to minimize in-culture variability. NaCl or KCl (250 mM) was added to experimental cultures, and an equivalent volume of sterile distilled water was added to control cultures. The time of stressor addition was recorded as T0 and samples were taken at 30, 60, 120, and 240min post exposure. The longest time point (< 5 h) was less than one-generation time, such that all samples were collected prior to stationary phase. Samples were chilled to 4°C in < 15sec during collection by pulling sample from production cultures through 7m of capillary tubing immersed in an ice bath using a peristaltic pump. Chilled samples were centrifuged, pellets washed with 4°C degassed sterile PBS and centrifuged again at 6000 x *g* (10min at 4°C). The final pellet was flash frozen in liquid N_2 and stored at -80°C. For each biomass production, the following purity and growth characteristics were recorded: temperature, pH, OD_{600}, AODC, sFTIR, total protein, anaerobic colony morphology and absence of aerobic colonies, and PLFA biosignatures.

Osmoprotection assays *D. vulgaris* was cultured anaerobically in LS4D. Stressors, osmolytes and other metabolites were added as indicated and growth was monitored via OD_{600} and by total cell protein.

Microarray analysis Oligonucleotide probe design and microarray construction were described previously (32). After RNA extraction, purification, and labeling, reverse transcription reaction was used to generate labeled cDNA probes. Labeled genomic DNA (Cy3) was used as control and the common reference to co-hybridize with labeled RNA (Cy5) samples for each slide. Each comparison was done in triplicate. Finally, with duplicate arrays on a given slide and three biological replicates, each gene has a total of 18 possible spots. Hybridized microarray slides were scanned using ScanArrayTM Express microarray analysis system (Perkin Elmer®, MA). Spot signal, spot quality, and background fluorescent intensities were quantified with ImaGene version 5.5 (Biodiscovery Inc., Los Angeles, CA).

Computational *Gene models:* TIGR models (NCBI) were used. *Microarray data analysis:* Log expression levels including global normalization were first computed for each microarray. Log expression levels from replicate arrays were averaged. Each gene was represented by two spots on each microarray, and spots flagged by the scanning software were excluded. Net signal of each spot was calculated by subtracting background and adding a pseudo-signal of 100 to enforce a positive value. For resulting net signals < 50, a value of 50 was used. For each spot, the expression level was a ratio of

the two channels, mRNA over genomic DNA. For each replicate, levels were normalized such that total expression level over the spots that were present on all replicates was identical. Finally, mean expression levels and standard deviations of each spot were calculated, requiring n > 1. To estimate differential gene expression between control and treatment conditions, normalized log ratios were used. The log ratio is $\log_2$(treatment) - $\log_2$(control). This log ratio is normalized using LOWESS on the difference vs. the sum of the log expression level (15). Sector-based artifacts were observed, therefore, the log ratio was further normalized by subtracting the median of all spots within each sector. Up to this point, data was processed using spots instead of genes to allow sector-based normalization. Finally, the spots for each gene were averaged to give a final normalized log ratio. To assess significance of the normalized log ratio, a z-score was calculated by the following equation:

$$Z = \frac{Log_2(Treatment/Control)}{\sqrt{0.25 + \sum \text{var}iance}}$$

where 0.25 is a pseudo-variance term.

Metabolite assays using Capillary electrophoresis Mass Spectrometry (CE-MS)

Three identical 50 ml cultures were pooled anaerobically and centrifuged at 10,000 x *g* (10min at 4^{o}C). The pellet was resuspended in 5ml cold methanol (kept on dry ice for >1 h) by vortexing and allowed to stand for 5 min on dry ice. A mixture of 5ml chloroform (Acros) and 1.925ml water was added to the lysate and mixed thoroughly to remove free phospholipids. The extraction mixture was centrifuged at 7000 x *g* for 5min to separate aqueous from non aqueous layers. The top layer was transferred to a 5000 MW cut-off filter (Vivaspin6®) and centrifuged at 7000 x *g* (10min at 4^{o}C). The filtrate was

lyophilized, reconstituted in 4 ml water, desalted using a 1g C18 cartridge (Varian) and lyophilized. Dried samples were reconstituted to produce the metabolite mixture in 100 µl buffer containing 115µM methionine sulfone as the internal standard. Data were obtained with positive ion mode via CE (Agilent) and analyzed using Electrospray MS (Agilent MSD). The metabolite mixture was resolved on a 1m x 50 µm fused silica column (Polymicro Technologies) with 1 M formic acid as electrolyte and 5 mM ammonium acetate as sheath liquid. Metabolites were identified by comparing the nominal mass and retention time compared with those of standards. Quantities of selected metabolites were estimated relative to the quantity of the known amount of internal standard. All reagents used were HPLC grade.

Isotope coded affinity tagging (ICAT) and tandem Liquid Chromatography Mass Spectrometry (LCMS) Cell pellets from 300 ml cultures at OD_{600} 0.3-0.4 were lysed in 2ml of 50 mM Tris-HCl, pH 8.0, by sonication on ice. Lysates were clarified by centrifugation at 14000 x *g* (30min at 4°C) and protein levels were determined using the BCA assay (Pierce). Samples of 300µg total cell protein from control and stressed samples (Time 120min) were ICAT labeled with light or heavy tags respectively as per manufacturer's instructions (Applied Biosystems). Trypsinised samples were desalted, dried, dissolved in 40µl 0.1% (vol/vol) 1 M formic acid and resolved via two-dimensional nano-LC using an inline strong cation exchange cartridge into salt cuts (5, 20, 30, 40, 50, 1000 mM KCl) and further resolved by reverse-phase separation (15 cm 300Å diameter C18 RP column, Dionex). A 0-30% gradient in the organic phase (80% ACN 0.1% 1 M formic acid) was used. The m/z of the resolved peptides was determined

using electrospray ionization and a time-of-flight mass spectrometer (QSTAR® Hybrid Quadrupole TOF, Applied Biosystems). TOF MS and MS/MS were analyzed using the ProICAT software (Applied Biosystems). The acquired data were searched against a theoretical database created using the FASTA file containing the ORFs from *D.vulgaris* Hildenborough, *E.coli* K12 and *B.subtilis* 168. Mass tolerance of 0.3 for MS and 0.3 for MS/MS were used to obtain the list of candidate proteins. Only proteins identified at >99% confidence were taken. Of these only those with Stressed: Control (heavy: light) quantitation quality > 75% were used. The ICAT strategy has been established to be very accurate for small changes, detecting as little as a 30% change in protein levels (3, 59). H:L ratios from peptides associated with the same protein were used to assess internal error in a manner similar to that described previously (21). The error was determined to be 29%, and therefore only changes greater than 29% were considered significant. For a complete list see supplementary data.

3D-nano-LC-MS/MS 3D proteomics, conducted at Diversa Corp., used fractionation of total proteins by three-dimensional LC followed by MS/MS analysis to identify the proteins as described previously (57). Replicate cultures from a control (time 0, 120min) and stressed sample (120min) were used to obtain total protein. Relative abundance of proteins in each sample was estimated based on the hypothesis that more abundant a peptide ion is in the mixture, the more likely this peptide ion is sampled during the course of the MS/MS experiment (33, 59). Using this model, total numbers of qualified spectral counts represent relative abundance of each protein under a specific condition. To identify proteins that have significant changes under different conditions, statistical

"local-pooled-error" test (27) was used. Only changers with $p < 0.05$ were considered to be significantly changed. 1356 proteins were identified in all samples and 47 showed reproducible changes between the control and stressed sample (supplementary data).

PLFA assays Pellets from 40 ml cultures (centrifuged at 1015 x *g* for 15min) were stored at -20ºC. Total lipids were extracted from the pellet with a modified Bligh-Dyer solution (58). Phospholipids were separated from total lipids on C18 silicic acid column (Unisil, Clarkson Chemical), methylated and then analyzed on an Agilent 6890N GC equipped with a flame-ionization detector. Peak confirmation was accomplished via MS (Agilent 5972A MSD), and double bond position confirmed with a dimethyl disulfide derivatization. Peak quantification was accomplished using an internal 19:0 FAME standard (Sigma).

sFTIR All sample handling was anaerobic at 4^{o}C. Cells were washed in ice-cold, oxygen-free buffer (0.1 M Tris-HCl, pH 7.5, 1.0 mM EDTA) and placed on a gold-coated microscope slide. Free-flowing buffer solution was removed and cells were placed inside a sample holder, which maintained a 100% relative humidity and anaerobic atmosphere. The ZnSe window of the sample holder allows IR spectra acquisition. IR measurements were conducted at the Advanced Light Source facility, LBNL, using the FTIR interferometer bench (Nicolet Magna 760) equipped with an IR microscope (Nic-Plan IR Microscope) as described earlier (26). Signals in the 4000-250cm^{-1} spectral region were interpreted using previously described principles (9). Characteristic CO_2 peaks and water vapor fingerprints were removed from the spectra, then normalized against the amide I

absorption peak (1648cm^{-1}). Each spectrum was the average of 20 raw spectra, and each raw spectrum represented at least 20 cells. Differences in spectra, which demonstrate difference in cellular changes of control vs. stressed biomass, were analyzed.

Results and Discussion

The defined LS4D medium used in our study contains sodium lactate as carbon source and electron donor and sodium sulfate as terminal electron acceptor. An additional 250 mM NaCl reduced the maximal growth rate of the *D. vulgaris* culture by 50% and had the striking phenotype of a five-fold elongation of cells in late log phase (Fig 1).

In this study, *D. vulgaris* cultures at mid-log phase were exposed to salt stress using 250 mM NaCl, and changes in gene expression were monitored at 30, 60, 120 and 240 min. A replicate experiment at 120 min was used to generate biomass for microarray analysis, proteomics, metabolite assays and macromolecule composition. The resulting data were used to delineate primary cellular responses to excess NaCl. Data from the KCl microarray were used to identify responses specific to excess Na^+ ions.

Accumulation of compatible solutes

The *D. vulgaris* genome encodes a putative GB/choline/proline ABC transport system. The three-gene operon contains *proV*, encoding an ATP-binding protein; *opuBB*, encoding a permease protein; and *proW*, encoding the periplasmic binding protein that serves as the substrate receptor in the transporter complex. Microarray analysis showed mRNA levels of all three genes to be highly up-regulated in response to both excess NaCl

and KCl (Fig 2). ICAT proteomics data for the same biomass supported *opuBB* up-regulation (Fig 3) and OpuBB was among the mostly highly up-regulated protein.

Surprisingly, even though no GB is present in LS4D medium, analysis of cell extracts using CE-MS showed GB to be present in both control and salt stressed biomass. Consistent both with microarray and proteomics observations, GB levels were higher in salt stressed biomass (Fig 3). Bacteria are known to scavenge GB present as contaminant in carbon sources (19). LS4D does contain choline, which can serve as a precursor to GB in a two-step process requiring an aldehyde dehydrogenase and an alcohol dehydrogenase (11), genes that are present in *D. vulgaris*, though microarray data did not identify any specific candidates.

In osmoprotection assays, very small concentrations of GB efficiently alleviated not only the growth inhibition due to excess salt but also prevented the late log phase cell elongation (Fig 1). Even though GB is an effective osmoprotectant, the up-regulated permease *opuBB* may not be specific for GB. Hence additional substrates/precursors known to be effective osmoprotectants were examined in *D. vulgaris* salt stress assays. Results show that choline does not alleviate salt stress in *D. vulgaris* (Fig 1). This may either be due to the inability of *D. vulgaris* to import choline, or absence of specific dehydrogenases that convert it to GB. GB has also been reported to be synthesized via sequential methylation of the glycine amino group by methyltransferases (42). Although several methyltransferases are annotated in *D. vulgaris*, addition of glycine, methyl glycine, or dimethyl glycine to salt-stressed cells showed no significant improvement in growth (supplementary data). Organisms that use GB as an osmoprotectant, *e.g.*, *E. coli*

and *B. subtilis*, can often synthesize it (11, 19). However, similar to *Lactobacillus spp*. (19), *D. vulgaris* uses GB exclusively via import.

Proline, a well documented osmoprotectant (4, 11) could be accumulated via up-regulation in biosynthesis, increased transport, or decreased proline oxidation to glutamate. Up-regulation of proline biosynthesis genes was not observed upon salt stress (supplementary data). Furthermore, CE-MS analysis indicated that cells did not accumulate proline during salt stress while glutamate levels did increase (Fig 3). In osmoprotection assays, proline did alleviate salt stress, but not as effectively as GB (Fig 1). Therefore despite the homology between the *B. subtilis* and *D. vulgaris opuBB*, proline appears not to be the preferred osmoprotectant for *D. vulgaris*.

In contrast, ectoine alleviated salt stress in concentrations comparable to that of GB (Fig 1). Interestingly, neither an ectoine biosynthesis pathway nor any ectoine-specific transport systems are annotated in *D. vulgaris*, though it is evident that uptake and accumulation of small polar osmolytes is a major salt stress response in *D. vulgaris*.

Among other amino acids, mRNA levels of tryptophan biosynthesis genes were markedly up-regulated in NaCl stress and to a lesser extent in KCl stress (supplementary data). We found no reports of tryptophan up-regulation in relation to salt or osmotic stress in other bacteria and have no explanation for this phenomenon. Addition of tryptophan to the growth medium did not alleviate salt stress (supplementary data).

Efflux of excess salt ions

D. vulgaris contains more than 14 genes annotated for cation/multidrug efflux (Fig 2, supplementary data) that may pump cations out of the cell using the same

mechanism as Na^+/H^+ antiporters. Genes in the three-gene operon (DVU2815-17) as well as a two-gene multidrug efflux operon (DVU3326-27) were highly up-regulated upon salt stress (Fig 2). A putative *acrAB* system (DVU0058-63) was highly up-regulated throughout the stress treatment in response to both NaCl and KCl (Fig 2), a phenomenon also observed in *E. coli* in response to 0.5 M NaCl (37). From the large number of up-regulated genes with cation/multidrug efflux domains, we infer that efflux systems play a major role in actively pumping excess salt ions out of the cell in *D.vulgaris*.

Several highly conserved Na^+/H^+ antiporters are also present in *D. vulgaris*, but for most examination of transcripts and protein profiles indicated no change in stressed cells (supplementary data). As these transcripts were present abundantly (unpublished observation, Huang and Alm), antiporters may effect salt efflux with no further up-regulation. One exception was the ubiquinone oxidoreductase subunit, *echA* (DVU0434), which showed increased transcript levels in both NaCl and KCl stressed cells (Fig 2). These oxidoreductases have been implicated in respiration coupled Na^+ efflux in several other bacteria (44, 47).

Down-regulated genes included those with Na^+ uptake, such as flagellar systems (Fig 2), suggesting that *D. vulgaris* would eventually become non-motile under salt stress. Similar down-regulation of the flagellar assembly genes has been observed in other bacteria, including *Shewanella oneidensis* (34) and *B.subtilis* (53). However, unlike *S. oneidensis*, the *D. vulgaris* cells were observed to be highly motile after salt stress (data not shown) and several key chemotaxis genes, such as *cheY* (DVU2073), were significantly and reproducibly up-regulated within 30 min of treatment with either NaCl or KCl (Fig 2). While *cheY* remained up-regulated throughout the later time points

monitored (Fig 2), other chemotaxis genes (*cheA*, *cheW*, *cheD*) were most highly up-regulated only at earlier time points (30 and 60 mins) (Fig 2). Up-regulation of chemotaxis genes may be indicative of an initial response in cells to move away from the stressful cations.

At the proteome level several periplasmic-binding proteins of ABC transport systems were significantly down-regulated (Table 1). While both proteomics techniques used in our study revealed this down-regulation, only one of these candidates showed a similar change at the mRNA level (DVU1937, supplementary data). Whether the down-regulation of periplasmic proteins is beneficial during salt stress requires further investigation.

Salt stress amelioration mechanisms

The most up-regulated protein identified in the salt stressed sample was the RNA helicase DVU3310 (Fig 2, Table 1), a DeaD/DeaH box binding protein known to facilitate RNA melting (17). Both RNA and DNA helicases confer tolerance to salt (46, 50), presumably by overcoming the effect of excess intracellular cations on RNA and DNA melting. Microarray data showed up-regulation in another RNA helicase as well as two DNA helicases (*dnaB* and *ruvB*) that form part of the DNA replication fork (Fig 2), indicating that stability of both RNA and DNA may have been affected by excess cations during salt stress.

Salt stress is known to affect fluidity of the cell wall, and lipid regulation plays a role in cell wall fluidity (35). Eight PLFAs constituting 80% of the total *D. vulgaris* PLFA composition (16) were used to observe the effect of NaCl stress on the PLFA

profile (Fig 4). Since our study did not addressed the long term adaptation to salt stress, no drastic changes were observed either in total PLFA content or the net contribution of each individual PLFA (supplementary data). However, changes that were observed during salt stress were not observed in the control biomass over the same period of time (Fig 4). The branched, unsaturated PLFA i17:1ω9c, that accounted for 14% of the total PLFA content and is characteristic of *Desulfovibrio* species (16), increased in stressed but not in control cells. In contrast, unbranched, saturated PLFAs 16:0 (7%) and 18:0 (25%) increased in control cells but not in salt-stressed cells. In general, branched PLFAs increased more in stressed than in unstressed cells.

Response of PLFA profile to salt stress has been examined in several bacteria (29, 35). Models for lipid composition changes in both Gram-positive and Gram-negative bacteria have been suggested (29). *D. vulgaris* appears to exhibit the mechanisms found generally in halotolerant, Gram-positive bacteria, wherein an overall increase in branched PLFA, both saturated and unsaturated, is observed during salt stress. Though it is the combined ratio of different PLFAs that determine viscosity of the resulting membrane, increases in lower-melting branched or unsaturated fatty acids are known to increase membrane fluidity (29). Salt, similar to cold stress, is known to increase membrane rigidity (35) and increases in branched PLFAs may be the bacterial response needed to re-establish optimal membrane fluidity. Consistent with this hypothesis, unsaturation in fatty acids also increases membrane fluidity and *Synechocystis* strains overexpressing a desaturase gene were found to be more robust under salt stress conditions (1).

The small increase in lipids in the salt-stressed biomass was also observed in sFTIR experiments of whole cells (Fig 4). No significant changes could be identified in

the expression of genes encoding biosynthesis or modification functions for fatty acids or polysaccharides (supplementary data). However, ICAT proteomics did reveal an increase in OmpH, putatively involved in lipopolysaccharide biosynthesis, and RfbA, involved cell wall biogenesis (Table 1).

Energy production

GB import, ion efflux, and helicases all require ATP hydrolysis for function which may explain the significant up-regulation in F-type ATPases (Fig 2, Table 1). Consistent with an increase in the energy requirement, expression of all genes (DVU0531- 36) in the operon encoding the high molecular weight cytochrome Hmc increased (Fig 2). Hmc is a potential transmembrane redox protein complex reported to be involved in electron transport and energy production (24). Interestingly, expression of the Rrf12 operon (DVU0529-30) located immediately downstream and the predicted negative regulator for Hmc (30), also increased during the salt stresses (supplementary data).

The six gene operon (DVU0846-51) encoding part of the sulfate reductase pathway was also up-regulated (supplementary data). At the protein level, ApsA, the adenylyl sulfate reductase α subunit (DVU0847) and QmoB, the Quinone-interacting membrane-bound oxidoreductase (DVU0849), appeared mildly up-regulated, though QmoA (DVU0848, also identified) did not show significant up-regulation (Table 1). Sulfate is the terminal electron acceptor for anaerobic respiration of *D. vulgaris.* The increases in expression of proteins for sulfate reduction suggest that stressed cells may require more energy than unstressed cells. In addition, the mRNA level for the sulfate

permease (DVU0279) was up-regulated. This may cause a paradox for the salt-stressed cell, since this permease has been shown to function as a Na^+ symporter (13).

An unexplained contradiction appears with the apparent down-regulation of lactate permeases in both NaCl and KCl stressed cells (Fig 2). Additional energy requirements would be expected to necessitate greater lactate uptake. Preliminary data from enzymatic assays conducted on cell culture supernatant did not show a change in lactate consumed by salt stressed cells (data not shown), but more experiments are required for a better understanding of lactate metabolism. The pyruvate metabolic pathway also appeared to be down-regulated (Fig 2, Table 1). However sufficient redundancy in the pyruvate to acetyl-CoA pathway exists in the genome so that this metabolic flux could have remained unchanged during salt stress.

Comparison of stress response to Na^+ vs. K^+

In many bacteria, K^+ accumulation via the *trk* and *kdp* systems is a primary response to excess Na^+ ions (7, 34, 39, 52). *D. vulgaris* has four genes (DVU0412-13, DVU1606, DVU2302) predicted to be involved in K^+ uptake and transport and an operon homologous to the *E. coli kdp* K^+ transport system (DVU3334-39). However, microarray data did not show significant change in any of these candidates except DVU1606, which increased in NaCl stress (supplementary data). Addition of KCl did not alleviate the detrimental effect of NaCl on growth. Infact increasing K^+ concentrations were found to be additive with Na^+ in decreasing growth rate (data not shown). Thus at the NaCl concentration used here, uptake of K^+ ions was not an important response mechanism in *D. vulgaris*.

Microarray data from NaCl and KCl challenges to *D. vulgaris* were striking in their overall similarity (Fig 2, (supplementary data)). Very few differences were observed but included the RNA helicase, DVU0256, up-regulated only in response to NaCl but not KCl (Fig 2), suggesting specificity to Na^+ ions. Several phage-related proteins, such as holin (DVU0202), also increased expression only during NaCl stress (supplementary data). Conversely, an ABC transport protein for branched amino acids (*DVU*2744) and several genes for methionine and leucine biosynthesis were up-regulated only in KCl stress (supplementary data).

Regulatory systems

Of the several regulons identified in *D. vulgaris* (49), the most striking differential expressions were the increases in gene expression for members of the ferric uptake regulon (FUR) after salt stress (Fig 2). FUR derepression was also observed in response to heat shock, oxygen exposure, and acid stress (He and Zhou, unpublished data) and might be a global stress response in *D. vulgaris*. In *B. subtilis*, high salinity causes iron deficiency, leading to derepression of FUR genes, in particular siderophore biosynthesis (25). Possibly because of its anaerobic lifestyle, *D. vulgaris* appears to lack a siderophore biosynthetic pathway. However, omission of Fe^{2+} from LS4D did not affect net sensitivity of *D. vulgaris* to salt or the ability of GB to alleviate growth deficiency (supplementary data). Surprisingly, in a *Δfur* mutant of *D. vulgaris*, addition of GB could not alleviate the growth deficiency conferred by salt stress but did reduce cell elongation (Bender and Wall, unpublished data).

In bacteria, two component systems play an important role in initiating response to external stimuli and stress. In the cyanobacterium *Synechocystis*, a histidine kinase involved in salt stress response has been identified (45). Microarray data of *D. vulgaris* transcripts showed changes in several histidine kinases during salt stress (supplementary data), but further experiments are needed to confirm their specific involvement. Other regulatory proteins, such as the stationary phase RpoS σ^{70} sigma factor, are also reported to be involved in salt stress response (12). Although some δ-proteobacteria apparently have a well-recognized RpoS ortholog (41), *D. vulgaris* appears not to encode RpoS. Three putative σ^{70} factors in *D. vulgaris*, *rpoD* (DVU1788), *rpoH* (DVU1584), and *fliA* (DVU3229), did not show significant change during NaCl stress, though σ^{54}, encoded by *rpoN* (DVU1628), was significantly up-regulated (supplementary data). Curiously, proteomics data also indicated that RpoC, the RNA polymerase β' subunit, increased in the salt stressed cells (Table 1).

Comparison of genomics data.

The microarray and proteomics studies conducted in this study were targeted to study stress response rather than adaptation. To ensure that stress would be measured but also that the cells were not moribund, the parallel studies were conducted at 2 hours following salt addition. While the expression levels for many genes were significantly were changed, most of the changes at the microarray level did not exceed five fold. This is not surprising since the doubling time for *D.vulgaris* growing in LS4D at 30^{o}C is 5 hours. The data suggest that changes at the proteome level were even milder. Using the cysteine tagging ICAT method, 167 proteins were identified and 139 had Stressed:

Control ratios. Of these 79 candidates showed changes greater than 30% and 27 showed trends similar to that of mRNA levels (supplementary data). Differences between microarray and proteomics data have been observed in most studies that attempted to use both to map cellular responses (3, 20, 23). These differences may arise because of the inherent lag between mRNA changes and changes in protein levels. Post transalational modifications and regulation, such as turnover and protein secretion, can also contribute to these differences. However, further validation is required to confirm the cause or significance of any of these differences. Additionally, while a correlation between absolute protein quantity and mRNA value may be expected (33, 56), correlations between fold changes in microarray vs. proteomics data appear more variable (3, 20, 23).

Salt stress model in *D.vulgaris* Hildenborough

The different techniques used in this study allowed us to observe the initial effects and responses to salt stress, and formulate a more complete salt stress model in a single organism (Fig 5). Uptake of available molecules from the environment, such as GB and ectoine, presents a robust strategy to counter osmotic stress, and appears to be the favored mechanism in *D. vulgaris*. The cells also initiated up-regulation of a variety of efflux mechanisms. However cells may also utilize available protective mechanisms such as Na^+/H^+ antiporters that are abundantly present but show no up-regulation upon stress. Other immediate responses include up-regulation of chemotaxis systems and apparent motility of the cells, adjustments in cell wall composition, and increases in ATP production and electron channeling. The most striking, long-term effect of salt stress is elongation of the cells, which may be caused by inhibition of DNA replication. While

additional experiments are required to confirm this hypothesis, our preliminary observations showed dilution in total DNA, and increase in the protein/DNA ratio in stressed cells. Increases observed in proteins required for melting base pairing is also consistent with this hypothesis. We infer from our assays that the uptake of osmolytes corrects these stress effects, setting the stage for further experiments to define the mechanism of osmoprotection.

Acknowledgements

This work was part of the Virtual Institute for Microbial Stress and Survival (http://vimss.lbl.gov) supported by the U. S. Department of Energy, Office of Science, Office of Biological and Environmental Research, Genomics:GTL Program through contract DE-AC02-05CH11231 with LBNL. We thank Keith Keller and Janet Jacobsen (LBNL) for the supplementary data website and Sherry Seybold (LBNL) for graphics support on Fig 5. Oak Ridge National Laboratory is managed by University of Tennessee-Battelle LLC for the Department of Energy under contract DE-AC05-00OR22725.

References:

1. **Allakhverdiev, S. I., M. Kinoshita, M. Inaba, I. Suzuki, and N. Murata.** 2001. Unsaturated fatty acids in membrane lipids protect the photosynthetic machinery against salt-induced damage in *Synechococcus*. Plant Physiol **125:**1842-53.

2. **Alm, E. J., K. H. Huang, M. N. Price, R. P. Koche, K. Keller, I. L. Dubchak, and A. P. Arkin.** 2005. The MicrobesOnline Web site for comparative genomics. Genome Res **15:**1015-22.

3. **Baliga, N. S., M. Pan, Y. A. Goo, E. C. Yi, D. R. Goodlett, K. Dimitrov, P. Shannon, R. Aebersold, W. V. Ng, and L. Hood.** 2002. Coordinate regulation of energy transduction modules in *Halobacterium sp*. analyzed by a global systems approach. Proc Natl Acad Sci U S A **99:**14913-8.

4. **Barron, A., G. May, E. Bremer, and M. Villarejo.** 1986. Regulation of envelope protein composition during adaptation to osmotic stress in *Escherichia coli*. J Bacteriol **167:**433-8.

5. **Benbouzidrollet, N. D., M. Conte, J. Guezennec, and D. Prieur.** 1991. Monitoring of a *Vibrio natriegens* and *Desulfovibrio vulgaris* marine aerobic biofilm on a stainless-steel surface in a laboratory tubular flow system. Journal of Applied Bacteriology **71:**244-251.

6. **Ben-David, E. A., P. J. Holden, D. J. Stone, B. D. Harch, and L. J. Foster.** 2004. The use of phospholipid fatty acid analysis to measure impact of acid rock drainage on microbial communities in sediments. Microb Ecol **48:**300-15.

7. **Bhargava, S.** 2005. The role of potassium as an ionic signal in the regulation of cyanobacterium Nostoc muscorum response to salinity and osmotic stress. J Basic Microbiol **45:**171-81.

8. **Blessing, T. C., B. W. Wielinga, M. J. Morra, and S. Fendorf.** 2001. CoIIIEDTA- reduction by *Desulfovibrio vulgaris* and propagation of reactions

involving dissolved sulfide and polysulfides. Environmental Science & Technology **35:**1599-1603.

9. **Brandenburg, K., S. S. Funari, M. H. Koch, and U. Seydel.** 1999. Investigation into the acyl chain packing of endotoxins and phospholipids under near physiological conditions by WAXS and FTIR spectroscopy. J Struct Biol **128:**175-86.

10. **Brandis, A., & R.K. Thauer.** 1981. Growth of Desulfovibrio species on hydrogen and sulphate as sole energy source. Journal of General Microbiology **126:**249-252.

11. **Bremer, R., and R. Kramer.** 2000. Coping with osmotic challenges: osmoregulation through accumulation and release of compatible solutes in bacteria,. ASM Press, Washington, D.C.

12. **Cheville, A. M., K. W. Arnold, C. Buchrieser, C. M. Cheng, and C. W. Kaspar.** 1996. rpoS regulation of acid, heat, and salt tolerance in *Escherichia coli* O157:H7. Appl Environ Microbiol **62:**1822-4.

13. **Cypionka, H.** 1995. Solute transport and cell energetics. Plenum, New York & London.

14. **Dimroth, P.** 1990. Mechanisms of sodium transport in bacteria. Philos Trans R Soc Lond B Biol Sci **326:**465-77.

15. **Dudoit, S., Fridlyand J.** 2002. A prediction-based resampling method for estimating the number of clusters in a dataset. Genome Biol. **3:**25.

16. **Edlund, A., P. D. Nichols, R. Roffey, and D. C. White.** 1985. Extractable and lipopolysaccharide fatty acid and hydroxy acid profiles from Desulfovibrio species. J Lipid Res **26:**982-8.

17. **Fairman, M. E., P. A. Maroney, W. Wang, H. A. Bowers, P. Gollnick, T. W. Nilsen, and E. Jankowsky.** 2004. Protein displacement by DExH/D "RNA helicases" without duplex unwinding. Science **304:**730-4.

18. **Funabashi, H., T. Haruyama, M. Mie, Y. Yanagida, E. Kobatake, and M. Aizawa.** 2002. Non-destructive monitoring of rpoS promoter activity as stress marker for evaluating cellular physiological status. J Biotechnol **95:**85-93.

19. **Glaasker, E., F. S. Tjan, P. F. Ter Steeg, W. N. Konings, and B. Poolman.** 1998. Physiological response of *Lactobacillus plantarum* to salt and nonelectrolyte stress. J Bacteriol **180:**4718-23.

20. **Griffin, T. J., S. P. Gygi, T. Ideker, B. Rist, J. Eng, L. Hood, and R. Aebersold.** 2002. Complementary profiling of gene expression at the transcriptome and proteome levels in *Saccharomyces cerevisiae*. Mol Cell Proteomics **1:**323-33.

21. **Griffin, T. J., D. K. Han, S. P. Gygi, B. Rist, H. Lee, R. Aebersold, and K. C. Parker.** 2001. Toward a high-throughput approach to quantitative proteomic analysis: expression-dependent protein identification by mass spectrometry. J Am Soc Mass Spectrom **12:**1238-46.

22. **Hadas, O., and R. Pinkas.** 1995. Sulfate reduction processes in sediments at different sites in lake kinneret, israel. Microbial Ecology **30:**55-66.

23. **Hanash, S. M., M. P. Bobek, D. S. Rickman, T. Williams, J. M. Rouillard, R. Kuick, and E. Puravs.** 2002. Integrating cancer genomics and proteomics in the post-genome era. Proteomics **2:**69-75.

24. **Heidelberg, J. F., R. Seshadri, S. A. Haveman, C. L. Hemme, I. T. Paulsen, J. F. Kolonay, J. A. Eisen, N. Ward, B. Methe, L. M. Brinkac, S. C. Daugherty, R. T. Deboy, R. J. Dodson, A. S. Durkin, R. Madupu, W. C. Nelson, S. A. Sullivan, D. Fouts, D. H. Haft, J. Selengut, J. D. Peterson, T. M. Davidsen, N. Zafar, L. Zhou, D. Radune, G. Dimitrov, M. Hance, K. Tran, H. Khouri, J. Gill, T. R. Utterback, T. V. Feldblyum, J. D. Wall, G. Voordouw, and C. M. Fraser.** 2004. The genome sequence of the anaerobic, sulfate-reducing bacterium *Desulfovibrio vulgaris* Hildenborough. Nat Biotechnol **22:**554-9.

25. **Hoffmann, T., A. Schutz, M. Brosius, A. Volker, U. Volker, and E. Bremer.** 2002. High-salinity-induced iron limitation in *Bacillus subtilis*. J Bacteriol **184:**718-27.

26. **Holman, H. Y., K. A. Bjornstad, M. P. McNamara, M. C. Martin, W. R. McKinney, and E. A. Blakely.** 2002. Synchrotron infrared spectromicroscopy as a novel bioanalytical microprobe for individual living cells: cytotoxicity considerations. J Biomed Opt **7:**417-24.

27. **Jain, N., J. Thatte, T. Braciale, K. Ley, M. O'Connell, and J. K. Lee.** 2003. Local-pooled-error test for identifying differentially expressed genes with a small number of replicated microarrays. Bioinformatics **19:**1945-51.

28. **Jebbar, M., L. Sohn-Bosser, E. Bremer, T. Bernard, and C. Blanco.** 2005. Ectoine-induced proteins in *Sinorhizobium meliloti* include an Ectoine ABC-type

transporter involved in osmoprotection and ectoine catabolism. J Bacteriol **187:**1293-304.

29. **Kates, M.** 1986. Influence of salt concentration on the membrane lipids of halophilic bacteria. FEMS Microbiol Rev **39:**95 -101.

30. **Keon, R. G., R. Fu, and G. Voordouw.** 1997. Deletion of two downstream genes alters expression of the hmc operon of *Desulfovibrio vulgaris* subsp. vulgaris Hildenborough. Arch Microbiol **167:**376-83.

31. **Ko, R., L. T. Smith, and G. M. Smith.** 1994. Glycine betaine confers enhanced osmotolerance and cryotolerance on Listeria monocytogenes. J Bacteriol **176:**426-31.

32. **Li, X., Z. He, and J. Zhou.** 2005. Selection of optimal oligonucleotide probes for microarrays using multiple criteria, global alignment and parameter estimation. Nucleic Acids Res **33:**6114-23.

33. **Liu, H., R. G. Sadygov, and J. R. Yates, 3rd.** 2004. A model for random sampling and estimation of relative protein abundance in shotgun proteomics. Anal Chem **76:**4193-201.

34. **Liu, Y., W. Gao, Y. Wang, L. Wu, X. Liu, T. Yan, E. Alm, A. Arkin, D. K. Thompson, M. W. Fields, and J. Zhou.** 2005. Transcriptome analysis of *Shewanella oneidensis* MR-1 in response to elevated salt conditions. J Bacteriol **187:**2501-7.

35. **Los, D. A., and N. Murata.** 2004. Membrane fluidity and its roles in the perception of environmental signals. Biochim Biophys Acta **1666:**142-57.

36. **Lovley, D. R., and E. J. P. Phillips.** 1994. Reduction of Chromate By *Desulfovibrio vulgaris* and Its C(3) Cytochrome. Applied and Environmental Microbiology **60**.

37. **Ma, D., D. N. Cook, M. Alberti, N. G. Pon, H. Nikaido, and J. E. Hearst.** 1995. Genes acrA and acrB encode a stress-induced efflux system of *Escherichia coli*. Mol Microbiol **16:**45-55.

38. **MacKay, V. L., X. Li, M. R. Flory, E. Turcott, G. L. Law, K. A. Serikawa, X. L. Xu, H. Lee, D. R. Goodlett, R. Aebersold, L. P. Zhao, and D. R. Morris.** 2004. Gene expression analyzed by high-resolution state array analysis and quantitative proteomics: response of yeast to mating pheromone. Mol Cell Proteomics **3:**478-89.

39. **Matsuda, N., H. Kobayashi, H. Katoh, T. Ogawa, L. Futatsugi, T. Nakamura, E. P. Bakker, and N. Uozumi.** 2004. Na+-dependent K+ uptake Ktr system from the cyanobacterium Synechocystis sp. PCC 6803 and its role in the early phases of cell adaptation to hyperosmotic shock. J Biol Chem **279:**54952-62.

40. **Noguera, D. R., G. A. Brusseau, B. E. Rittmann, and D. A. Stahl.** 1998. Unified model describing the role of hydrogen in the growth of *Desulfovibrio vulgaris* under different environmental conditions. Biotechnology and Bioengineering **59.:**732-746.

41. **Nunez, C., L. Adams, S. Childers, and D. R. Lovley.** 2004. The RpoS sigma factor in the dissimilatory Fe(III)-reducing bacterium *Geobacter sulfurreducens*. J Bacteriol **186:**5543-6.

42. **Nyyssola, A., T. Reinikainen, and M. Leisola.** 2001. Characterization of glycine sarcosine N-methyltransferase and sarcosine dimethylglycine N-methyltransferase. Appl Environ Microbiol **67:**2044-50.

43. **Ouattara, A. S., and V. A. Jacq.** 1992. Characterization of sulfate-reducing bacteria isolated from senegal ricefields. Fems Microbiology Ecology **101.:**217-228.

44. **Padan, E., and T. A. Krulwich.** 2000. Sodium stress in in bacterial stress response. ASM Press, Washington, D.C.

45. **Paithoonrangsarid, K., M. A. Shoumskaya, Y. Kanesaki, S. Satoh, S. Tabata, D. A. Los, V. V. Zinchenko, H. Hayashi, M. Tanticharoen, I. Suzuki, and N. Murata.** 2004. Five histidine kinases perceive osmotic stress and regulate distinct sets of genes in Synechocystis. J Biol Chem **279:**53078-86.

46. **Panepinto, J., L. Liu, J. Ramos, X. Zhu, T. Valyi-Nagy, S. Eksi, J. Fu, H. A. Jaffe, B. Wickes, and P. R. Williamson.** 2005. The DEAD-box RNA helicase Vad1 regulates multiple virulence-associated genes in *Cryptococcus neoformans*. J Clin Invest **115:**632-41.

47. **Pfenninger-Li, X., S. Albracht, R. van Belzen, and P. Dimroth.** 1996. NADH:ubiquinone oxidoreductase of *Vibrio alginolyticus* purification, properties, and reconstitution of the Na+ pump. Biochemistry **35:**6233-6242.

48. **Postgate, J. R.** 1984. The Sulfate-Reducing Bacteria. Cambridge University Press, Cambridge.

49. **Rodionov, D. A., I. Dubchak, A. Arkin, E. Alm, and M. S. Gelfand.** 2004. Reconstruction of regulatory and metabolic pathways in metal-reducing delta-proteobacteria. Genome Biol **5:**R90.

50. **Sanan-Mishra, N., X. H. Pham, S. K. Sopory, and N. Tuteja.** 2005. Pea DNA helicase 45 overexpression in tobacco confers high salinity tolerance without affecting yield. Proc Natl Acad Sci U S A **102:**509-14.

51. **Shapiguzov, A., A. A. Lyukevich, S. I. Allakhverdiev, T. V. Sergeyenko, I. Suzuki, N. Murata, and D. A. Los.** 2005. Osmotic shrinkage of cells of *Synechocystis sp*. PCC 6803 by water efflux via aquaporins regulates osmostress-inducible gene expression. Microbiology **151:**447-55.

52. **Sleator, R. D., and C. Hill.** 2002. Bacterial osmoadaptation: the role of osmolytes in bacterial stress and virulence. FEMS Microbiol Rev **26:**49-71.

53. **Steil, L., T. Hoffmann, I. Budde, U. Volker, and E. Bremer.** 2003. Genome-wide transcriptional profiling analysis of adaptation of *Bacillus subtilis* to high salinity. J Bacteriol **185:**6358-70.

54. **Steuber, J., C. Schmid, M. Rufibach, and P. Dimroth.** 2000. Na+ translocation by complex I (NADH:quinone oxidoreductase) of *Escherichia coli*. Mol Microbiol **35:**428-34.

55. **Tabak, H. H., and R. Govind.** 2003. Advances in biotreatment of acid mine drainage and biorecovery of metals: 2. Membrane bioreactor system for sulfate reduction. Biodegradation . **14:**437-452.

56. **Wang, R., J. T. Prince, and E. M. Marcotte.** 2005. Mass spectrometry of the *M. smegmatis* proteome: protein expression levels correlate with function, operons, and codon bias. Genome Res **15:**1118-26.

57. **Wei, J., J. Sun, W. Yu, A. Jones, P. Oeller, M. Keller, G. Woodnutt, and J. M. Short.** 2005. Global proteome discovery using an online three-dimensional LC-MS/MS. J Proteome Res **4:**801-8.

58. **White, C., Bobbie RJ, King JD, Nickels, JS, Amoe P. .** 1979. Lipid analysis of sediments for microbial biomass and community structure. American Society of Testing and Materials, Philadelphia, PA.

59. **Wolters, D. A., M. P. Washburn, and J. R. Yates, 3rd.** 2001. An automated multidimensional protein identification technology for shotgun proteomics. Anal Chem **73:**5683-90.

60. **Ye, Q., Y. Roh, S. L. Carroll, B. Blair, J. Zhou, C. L. Zhang, and M. W. Fields.** 2004. Alkaline anaerobic respiration: isolation and characterization of a novel alkaliphilic and metal-reducing bacterium. Appl Environ Microbiol **70:**5595-602.

Figure Captions.

FIG 1 Effect of salt stress on growth and cell morphology of *D. vulgaris* and role of osmoprotectants **A)** (i) effect of 250 mM additional NaCl or KCl on growth of *D. vulgaris* in LS4D medium and also effect of the presence of 2 mM GB during salt stress, (ii) effect of proline and choline on NaCl stressed cells, (iii) effect of ectoine on NaCl or KCl stressed cells. **B)** Scanning electron microscopy images of *D. vulgaris* grown in

different conditions as indicated (Electron Microscopy Core, University of Missouri, Columbia).

FIG 2 A) Selected hits from the NaCl and KCl time course microarrays. Candidates are grouped by function or gene ID numbers. **B)** Comparison of the changes in mRNA levels in 250 mM KCl stress (120min) on y-axis and in 250 mM NaCl stress (120min) on x-axis. Values on both axes are $\log_2$ of the ratio of mRNA level under stressed conditions to mRNA from control genomic DNA. The plot represents the large overlap between KCl and NaCl stress response. Points in the top right hand quadrant represent increases in both data sets. Highlighted data for selected candidates are labeled in the legend.

FIG 3 A) Heavy and light tagged MS parent ion peaks of the +2 charged peptide, FTCLGIR (mass = 1046.59), used to obtain relative peak quantification, stressed: control = 3.45 (Computed using ProICAT). FTCLGIR was sequenced at 99% confidence and used to ID OpuBB (DVU2298). **B)** Quantities of selected metabolites estimated relative to the internal standard (set at 100%). Values are averages of three technical replicates.

FIG 4 Fatty acid data **(A)** Relative change of eight major types of PLFA after NaCl stress (See supplementary data for fatty acid structures). Mole fractions of individual PLFAs were measured in triplicate. Data shown are computed as [(V1/V0)/(C1/C0) -1] where V is salt stressed and C is control. Time point 1 = 120min, 0 = 0min. **(B)** sFTIR data showing the 3400-2400 cm^{-1} window illustrating changes in the peaks at (a) 2925cm^{-1}

(b) 2958cm^{-1} (c) 2852cm^{-1} indicative of increase in total lipid content in the salt treated cells.

FIG 5 Schematic of molecular changes observed in *D. vulgaris* upon exposure to inhibitory NaCl concentrations. Symbols in red indicate an increase while those in blue indicate decrease. Gray indicates no change. (a) Data gathered from microarray, proteomics, metabolite and osmoprotection assays, (b) microarray and proteomics, (c) PLFA and FTIR analyses, and (d) microarray analysis only. Cell morphology data used electron microscopy.

Table 1. Selected proteomics data

DVU ID[a]	name	description	ICAT[b]	3D-nano-LC-MS/MS[c]	
ATP Synthesis			**log2(S:C)**	**log2(S:C)**	**p-value**
DVU0775	atpD	ATP synthase, F1 beta subunit	**1.03**	-0.11	0.8
DVU0777	atpA	ATP synthase, F1 alpha subunit	**0.58**	0.40	0.35
DVU0778	atpH	ATP synthase, F1 delta subunit	**0.74**	-0.64	0.29
ABC Transport binding proteins					
DVU0712	NA	amino acid ABC transporter, periplasmic-binding protein	**-1.41**	**-1.79**	**0.00**
DVU0745	NA	ABC transporter, periplasmic substrate-binding protein	**-0.81**		
DVU1937	NA	ABC transporter, periplasmic phosphonate-binding protein, putative	**-1.17**	**-1.23**	**0.01**
DVU2342	NA	amino acid ABC transporter, periplasmic amino acid-binding protein	**-1.07**	**-2.05**	**0.01**
DVU0547	NA	branched chain amino acid ABC transporter, periplasmic binding protein	**-1.33**	**-1.28**	**0.028**
Sulfate Reduction					
DVU0847	ApsA	adenylyl-sulphate reductase, alpha subunit	**0.57**	0.17	0.68
DVU0848	QmoA	Quinone-interacting membrane-bound oxidoreductase	0.21	-0.25	0.55
DVU0849	QmoB	Quinone-interacting membrane-bound oxidoreductase	**0.63**	0.23	0.59
Pyruvate -> Acetate					
DVU3025	poR	pyruvate-ferredoxin oxidoreductase	0.48	0.05	0.90
DVU3027	glcD	glycolate oxidase, subunit GlcD	-0.40	-0.26	0.55
DVU3028	NA	iron-sulfur cluster-binding protein	-0.02	**-1.71**	**0.00**
DVU3029	pta	phosphate acetyltransferase	-0.06	-0.66	0.13
DVU3030	ackA	acetate kinase	-0.35	-0.78	0.07
DVU3032	NA	conserved hypothetical protein	0.06	**-0.96**	**0.03**
Selected Changers					
DVU3310	deaD	ATP-dependent RNA helicase, DEAD/DEAH family	**2.24**	**3.08**	**0.00**
DVU2370	ompH	outer membrane protein OmpH, putative	**0.64**	-1.03	0.23
DVU3242	rpoZ	DNA-directed RNA polymerase, omega subunit	**0.66**	2.32	0.61
DVU0697	rfbA	mannose-1-phosphate-guanylyltransferase/mannose-6-phosphate isomerase	**0.75**	-0.50	0.59
DVU2929	rpoC	DNA-directed RNA polymerase, beta prime subunit	**0.58**	0.64	0.18
DVU0832	NA	tetrapyrrole methylase family protein	**-2.65**	-7.64	0.052
DVU2013	NA	hybrid cluster protein	**-0.61**	**-1.37**	**0.002**
DVU0979	b1200	DAK1 domain protein	**-0.75**	**-1.87**	**0.005**

S = stressed; C = control

[a] DVU ID descriptions can be found on microbesonline.org (2)

[b] ICAT: Shown data have ID confidence >99% , Quantitation score >75%; Change >29% is significant (bold)

[c] 3D-nano-LC-MS/MS estimates quantity via spectral count; p values < 0.05 are in bold

Figure 1

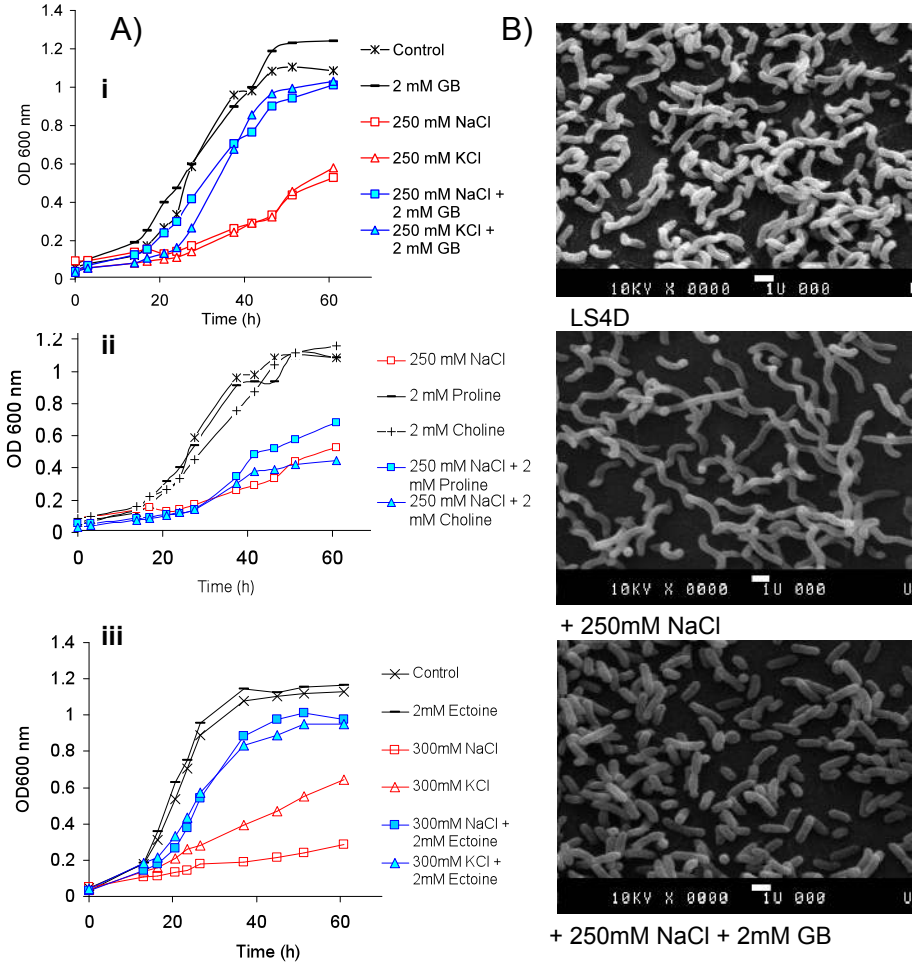
A)
i
OD 600 nm
Time (h)
Control
2 mM GB
250 mM NaCl
250 mM KCl
250 mM NaCl + 2 mM GB
250 mM KCl + 2 mM GB
ii
OD 600 nm
Time (h)
250 mM NaCl
2 mM Proline
2 mM Choline
250 mM NaCl + 2 mM Proline
250 mM NaCl + 2 mM Choline
iii
OD600 nm
Time (h)
Control
2mM Ectoine
300mM NaCl
300mM KCl
300mM NaCl + 2mM Ectoine
300mM KCl + 2mM Ectoine
B)
LS4D
+ 250mM NaCl
+ 250mM NaCl + 2mM GB

Figure 2

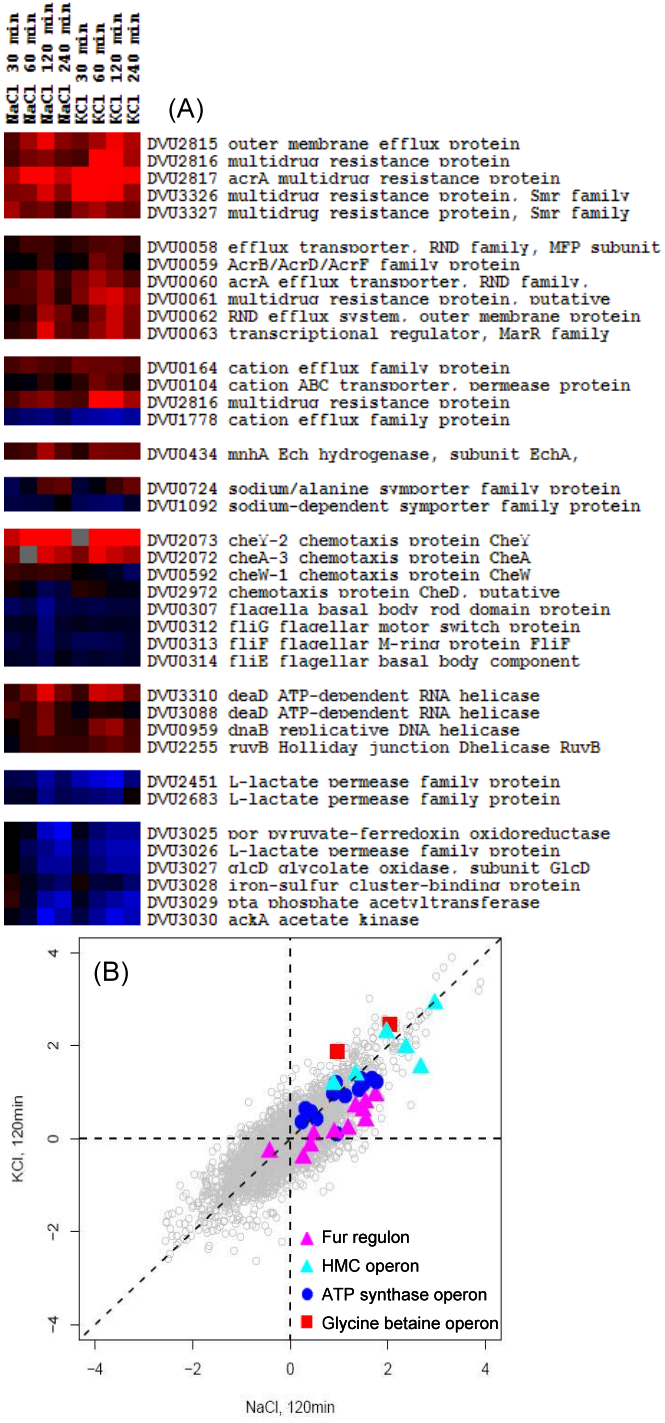
NaCl 30 min
NaCl 60 min
NaCl 120 min
NaCl 240 min
KCl 30 min
KCl 60 min
KCl 120 min
KCl 240 min
(A)
DVU2815 outer membrane efflux protein
DVU2816 multidrug resistance protein
DVU2817 acrA multidrug resistance protein
DVU3326 multidrug resistance protein, Smr family
DVU3327 multidrug resistance protein, Smr family
DVU0058 efflux transporter, RND family, MFP subunit
DVU0059 AcrB/AcrD/AcrF family protein
DVU0060 acrA efflux transporter, RND family,
DVU0061 multidrug resistance protein, putative
DVU0062 RND efflux system, outer membrane protein
DVU0063 transcriptional regulator, MarR family
DVU0164 cation efflux family protein
DVU0104 cation ABC transporter, permease protein
DVU2816 multidrug resistance protein
DVU1778 cation efflux family protein
DVU0434 mnhA Ech hydrogenase, subunit EchA,
DVU0724 sodium/alanine symporter family protein
DVU1092 sodium-dependent symporter family protein
DVU2073 cheY-2 chemotaxis protein CheY
DVU2072 cheA-3 chemotaxis protein CheA
DVU0592 cheW-1 chemotaxis protein CheW
DVU2972 chemotaxis protein CheD, putative
DVU0307 flagella basal body rod domain protein
DVU0312 fliG flagellar motor switch protein
DVU0313 fliF flagellar M-ring protein FliF
DVU0314 fliE flagellar basal body component
DVU3310 deaD ATP-dependent RNA helicase
DVU3088 deaD ATP-dependent RNA helicase
DVU0959 dnaB replicative DNA helicase
DVU2255 ruvB Holliday junction DNA helicase RuvB
DVU2451 L-lactate permease family protein
DVU2683 L-lactate permease family protein
DVU3025 por pyruvate-ferredoxin oxidoreductase
DVU3026 L-lactate permease family protein
DVU3027 glcD glycolate oxidase, subunit GlcD
DVU3028 iron-sulfur cluster-binding protein
DVU3029 pta phosphate acetyltransferase
DVU3030 ackA acetate kinase
(B)
KCl, 120min
NaCl, 120min
4
2
0
−2
−4
Fur regulon
HMC operon
ATP synthase operon
Glycine betaine operon

Figure 3

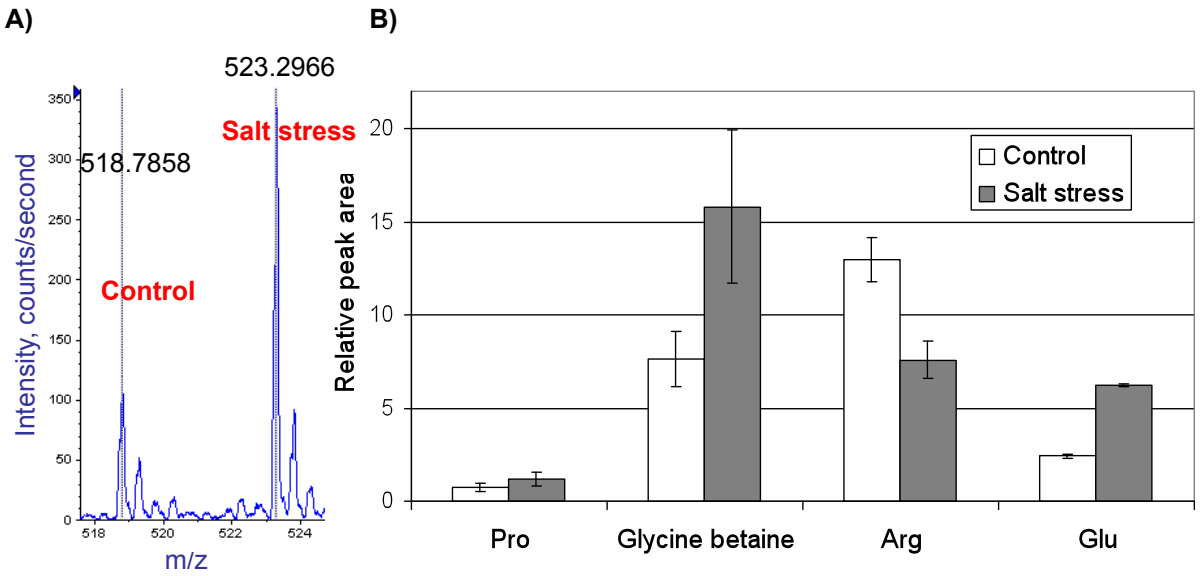
A)
B)
523.2966
Salt stress
518.7858
Control
Intensity, counts/second
m/z
Relative peak area
Control
Salt stress
Pro
Glycine betaine
Arg
Glu

Figure 4

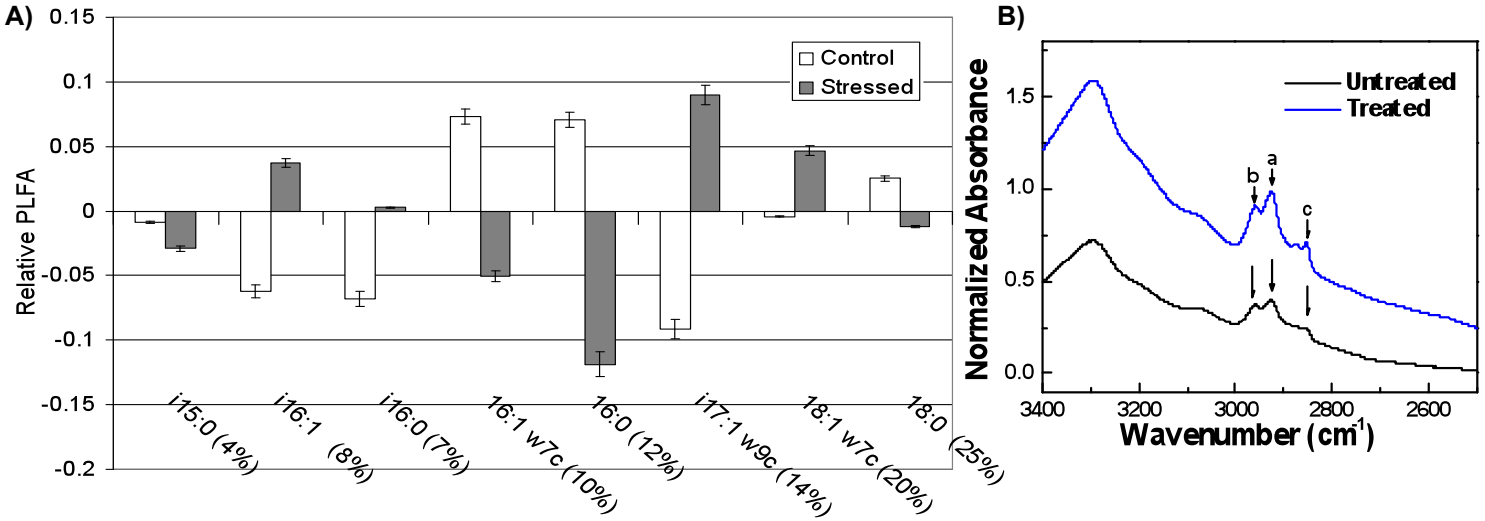
A)
Relative PLFA
0.15
0.1
0.05
0
-0.05
-0.1
-0.15
-0.2
Control
Stressed
i15:0 (4%)
i16:1 (8%)
i16:0 (7%)
16:1 w7c (10%)
16:0 (12%)
i17:1 w9c (14%)
18:1 w7c (20%)
18:0 (25%)
B)
Normalized Absorbance
1.5
1.0
0.5
0.0
Untreated
Treated
a
b
c
3400
3200
3000
2800
2600
Wavenumber (cm-1)

Figure 5

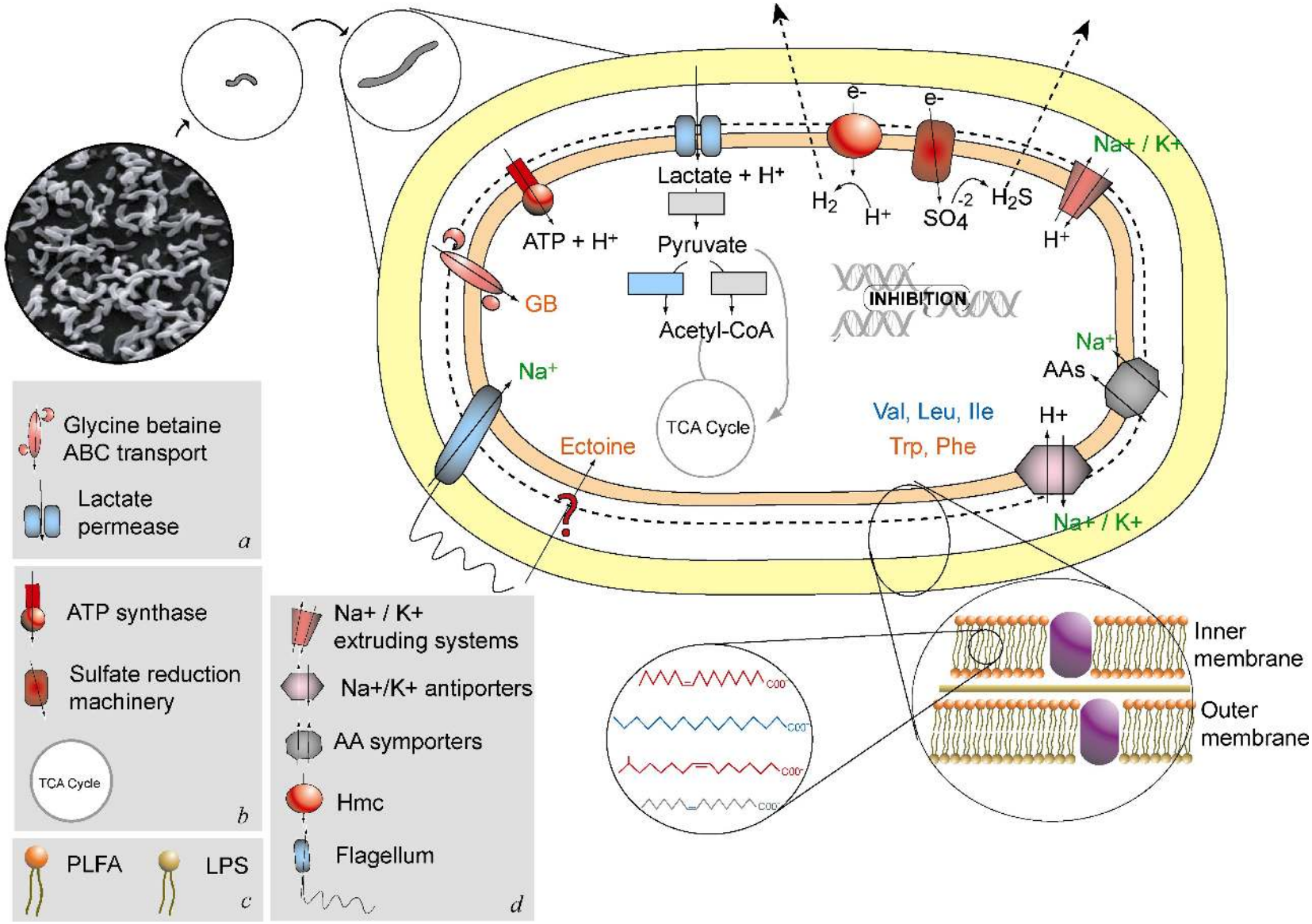
Lactate + H+
ATP + H+
Pyruvate
GB
Acetyl-CoA
INHIBITION
Na+
Ectoine
TCA Cycle
Val, Leu, Ile
Trp, Phe
e-
e-
H2
H+
SO4
-2
H2S
Na+ / K+
H+
Na+
AAs
H+
Na+ / K+
Inner membrane
Outer membrane
Glycine betaine ABC transport
Lactate permease
a
ATP synthase
Sulfate reduction machinery
TCA Cycle
b
PLFA
LPS
c
Na+ / K+ extruding systems
Na+/K+ antiporters
AA symporters
Hmc
Flagellum
d